JCTC Journal of Chemical Theory and Computation

pubs.acs.org/JCTC Article

"In Silico" Seawater

Ivan M. Zeron,[‡] Miguel A. Gonzalez,[‡] Edoardo Errani, Carlos Vega, and Jose L. F. Abascal*

Cite This: J. Chem. Theory Comput. 2021, 17, 1715−1725 Read Online

ACCESS | Metrics & More | Article Recommendations | Supporting Information

ABSTRACT: Many important processes affecting the earth's climate are determined by the physical properties of seawater. In addition, desalination of seawater is a significant source of drinking water for the human population living in coastal areas. Since the physical properties of seawater governing these processes depend on the molecular interactions among its components, a deeper knowledge of seawater at the molecular level would contribute to a better understanding of these phenomena. However, in strong contrast with the situation in other areas such as biomolecules or materials science, molecular simulation studies reporting the physical properties of seawater are currently lacking. This is probably due to the usual perception of the seawater composition being too complex to approach. This point of view ignores the fact that physical properties of seawater are dependent on a single parameter representing the composition, namely the salinity. This is because the relative proportions of any two major constituents of seasalt are always the same. Another obstacle to performing molecular simulations of seawater could have been the unavailability of a satisfactory force field representing the interactions between water molecules and dissolved substances. However, this drawback has recently been overcome with the proposal of the Madrid-2019 force field. In this work we show for the first time that molecular simulation of seawater is feasible. We have performed molecular dynamics simulations of a system, the composition of which is close to the average composition of standard seawater and with the molecular interactions given by the Madrid-2019 force field. In this way we are able to provide quantitative or semiquantitative predictions for a number of relevant physical properties of seawater for temperatures and salinities from the oceanographic range to those relevant to desalination processes. The computed magnitudes include static (density), dynamical (viscosity and diffusion coefficients), structural (ionic hydration, ion−ion distribution functions), and interfacial (surface tension) properties.

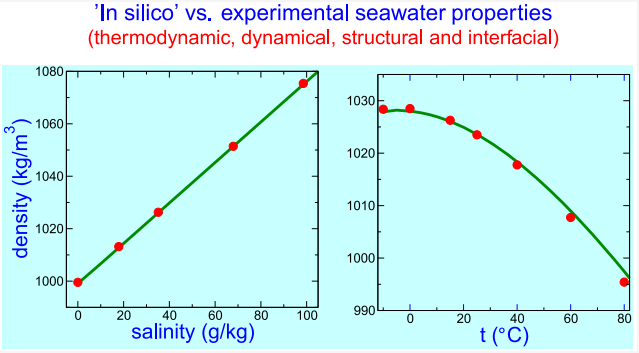

1. INTRODUCTION

Seawater is a complex solution of substances, mostly ions, in water. The complex composition of seawater is often perceived as a barrier to carry out numerical studies of its properties at the molecular level. In fact, molecular simulation studies reporting the physical properties of seawater are currently lacking. This is in strong contrast with the situation in other areas like biomolecules or materials science. While in these areas molecular simulation now plays an essential role as a complementary technique to experimental measurements, similar applications to investigate features of salty systems of difficult experimental access is much more limited. However, it is important to note that, despite the complexity of the seasalt composition, the most relevant physical properties of marine water —leaving aside surface or coastal effects— depend essentially on a single parameter representing the composition, namely the salinity. Salinity is then a fundamental property of seawater and basic to understanding biological and physical processes in oceans. The absolute salinity is defined as the total amount of dissolved substances (in grams) per kilogram of seawater.[1] The oceans salinity is usually between 31 and 38 g/kg but higher ranges are relevant to desalination processes.

The apparent contradiction between the complexity of seasalt composition and the fact that seawater properties are essentially dependent on the salinity can be easily explained. Irrespective of the total salinity, the relative proportions of any two major constituents of seasalt are always the same. This evidence is known from the beginning of the 19th century[2,3] and it is sometimes referred to as the Principle of Constant Proportions. The Principle of Constant Proportions allows the definition of a precise reference composition for Standard Seawater. The latter (arbitrary) definition was first proposed by Knudsen[4] and refers to certain surface seawater samples taken from the North Atlantic ocean. Currently, the Interna-

Received: January 20, 2021
Published: February 3, 2021

https://dx.doi.org/10.1021/acs.jctc.1c00072
J. Chem. Theory Comput. 2021, 17, 1715−1725

tional Association for the Physical Sciences of the oceans (IAPSO) oversees the preparation of Standard Seawater to ensure the quality and comparability of salinity data worldwide. In what follows we will simply refer to IAPSO Standard Seawater as seawater. In 2008, a Reference Composition—consisting of the proportions of components of seawater—was defined.[5] Salinity differences are then caused by either evaporating fresh water or adding fresh water from rivers and melted ice. In some way, this allows us to consider seawater as a two component mixture, seasalt and water, the salinity being the representative variable for the solution concentration.

The temperature of the oceans shows a characteristic vertical profile, called the thermocline, which depends on the latitude. Similar patterns are found for the salinity, the halocline. Since temperature and salinity determine the thermodynamic properties of seawater, density exhibits the same type of vertical profile as the thermocline and halocline. This means that seawater does not mix vertically. The mixing is produced by ocean currents, as shown for the first time by Sandstrom in 1908.[6] These currents give rise to the thermohaline circulation[7] which plays a decisive role on the Earth's climate[8] and on the marine biology. In this way, knowledge of the dependence of the density on the temperature and salinity of marine water is crucial for the understanding and modeling of the thermohaline circulation.

Thermophysical properties of seawater are well-known. In fact, there is a Gibbs function formulation, denoted as TEOS-10[9] from which all the thermodynamic properties of seawater can be consistently derived. Apart of the limited range of the variables concerned (temperature, pressure, and salinity) which are extended in other thermodynamics formulations[10] these equations are quite complex and do not allow a greater understanding of the role of the equation of state in the setting of the large-scale circulation. Although there are attempts to define simplified yet realistic equations of state for seawater,[11] we believe that molecular simulation is the ideal tool to get a better understanding of the thermodynamic properties of seawater.

Molecular simulation[12] has been recognized as a powerful tool to investigate the properties of molecular systems. It is complementary to experimental measurements and may be of great help in conditions under which performing an experiment is a challenging task.[13−15] However, to the best of our knowledge, it has never been used to investigate seawater. There are two likely reasons for that. First, it might seem that the complex seawater composition and its dependence on latitude and depth would prevent an investigation of global interest. Nevertheless, this point of view does not take into account the relative simplicity derived from the principle of constant proportions. Here we show that a system containing a reduced number of ions mimics very acceptably the mole fractions of seasalt as defined by the seawater Reference Composition and that the resulting system with added water is suitable for computer simulation.

On the other hand, molecular simulation relies on the availability of a good description of the interactions between ions and water. In recent years we have seen important advances regarding this topic.[16−21] As we will see below, the complexity of the seawater composition implies the simulation of considerably large samples. In these conditions, the use of polarizable models would require huge computational resources so we focus our interest on a rigid nonpolarizable model for water and molecular ions. A very fruitful idea has been the incorporation of the electronic continuum correction.[22] It has been argued that polarizable models can be reduced to nonpolarizable equivalent models with scaled charges.[23] Force fields based on this idea yielded an unprecedented agreement with the experimental properties of electrolyte solutions.[24−27] In 2017 we proposed a force field for NaCl in water[28] based on the widely tested TIP4P/2005[29,30] water model and the use of scaled charges for the ions. The success of this work prompted us to extend it and develop a force field, termed as Madrid-2019, including parameters for the more abundant ions of seawater.[31] We are thus in a good position to address the issue of investigating the properties of seawater from a molecular perspective.

In this work we study, using molecular simulation with the Madrid-2019 force field, the equation of state of seawater, that is, the dependence of density on temperature and salinity, $\rho = \rho(T, S)$. We also check the performance of the force field for other magnitudes representative of the thermophysical behavior of seawater. In particular, we have also evaluated dynamical (viscosity and diffusion coefficients), structural (ionic hydration, ion−ion distribution functions), and interfacial (surface tension) properties. It will be shown that the thermophysical properties of seawater can be satisfactorily predicted by molecular simulations with the Madrid-2019 force field.

2. "IN SILICO" SEASALT

The Reference Composition of Standard Seawater is *defined*[5] in terms of the mole fractions of the solute components with a precision of $1/10^7$. The number of water molecules required to produce a seawater sample with the Reference Composition and a salinity around 35 g/kg would then be of the order of 5×10^8. These numbers are obviously not adequate for computer simulation. It is also arguable that very minor components cannot significantly affect the physical properties of seawater. One of the goals of this work is to propose a simplified composition (which we term as "in silico" seasalt, ISSS) that enables a trustworthy comparison between simulation and experiment.

The first step is to shorten the list of components of seawater. For example, the simulation of a salty solution mimicking as close as possible the seasalt composition but containing just one CO_2 and one OH^- anion would still require around 7×10^7 water molecules. The six most abundant ions—chloride, sodium, sulfate, magnesium, calcium, and potassium—represent 99.7% of the seasalt mole fraction. The addition of two more ions to the list—bicarbonate and bromide—would elevate the percentage to 99.9%. It is important to note that constituents such as dissolved gases (CO_2, O_2) or inorganic salts (made of phosphorus or nitrogen) may play an essential role in climate regulation or in biological productivity but are irrelevant regarding the physical properties. In fact, neither O_2 nor any phosphorus or nitrogen compound form a part of the Reference Composition definition of seawater. A solution containing bicarbonate and bromide could indeed be tractable with current computer resources. However, the interaction potentials for these ions are presently much less reliable than those for the most abundant ions. We have thus decided at this stage to describe our "in silico" seasalt by including explicitly only the six ions mentioned above.

From the mole fractions and the ionic charge of the six components mentioned it is clear that the charge balance is not

https://dx.doi.org/10.1021/acs.jctc.1c00072
J. Chem. Theory Comput. 2021, 17, 1715−1725

Table 1. Composition of the "in Silico" Seasalt, ISSS, Used in This Work[a]

component	X_{ion}	mass	N_{ISSS}	X_{ISSS}	$M_{ISSS+water}$
chloride	0.4874839	19.35271	155	0.4874	19.349
sodium	0.4188071	10.78145	133	0.4182	10.766
sulfate	0.0252152	2.71235	8	0.0252	2.706
magnesium	0.0471678	1.28372	15	0.0472	1.284
calcium	0.0091823	0.41208	3	0.0094	0.423
potassium	0.0091159	0.39910	3	0.0094	0.413
minor components	0.0030278	0.22363	1	0.00314	0.222
sum	1.0000000	35.16504	318	1.0000	35.164
water		964.83496	15210		964.836

[a]To satisfy the electroneutrality of the solution, the charge of the "minor components" is the same as that of the chloride anions. Second column shows the mole fractions defined in the Reference Composition for solutes with $x > 0.002$[5]. Third column displays the amounts (g) of each component in the Reference Seawater at $S = 35.16504$ g/kg salinity. Fourth and fifth columns give the number of ions in the ISSS sample and their corresponding mole fractions. The last column presents the amounts (g) of each component in the ISSS + water system at $S = 35.165$ g/kg. A value of 63 g/mol is assumed for the molecular mass of the "minor components". With this choice, the average molecular mass of the ISSS seasalt is 31.404 g/mol, the same as that of the Reference Composition of Standard Seawater.

easily satisfied. This is related to the fact that most of the neglected constituents carry a negative charge. It is then convenient to include also a special type of solute by grouping together the mole fraction and charge of the minor components. This "minor components" solute would carry a negative charge, and its assigned molecular mass would be that required for the average molecular mass of the ionic sample to be the same as that of the Reference Composition, namely 31.4038218 g/mol.[5]

We have carried out a systematic search (see Supporting Information) looking for optimal sample sizes that reproduce as close as possible the Reference Composition with a minimum of solute molecules. Among them, we have arrived at a relatively small sample containing six types of ions and a total of 318 solute molecules (see Table 1). The sample, which will be referred to as ISSS, reproduces the Reference Composition mole fractions with a root-mean-square deviation around 0.0003. Table 1 shows the number of ions of each type and compares the molality of the components with the corresponding Reference Composition definition. It also shows the amounts of each component in the Reference Composition Standard Seawater and in the ISSS + water (318 ions +15210 water molecules) systems at $S = 35.165$ g/kg salinity. In the Supporting Information we give a detailed description of a number of optimal compositions for up to 13 seasalt components.

3. METHODS

In this work we use molecular dynamics simulation to investigate the properties of a system mimicking the composition of Standard Seawater. We have chosen the successful TIP4P/2005 model[29] to account for the interactions between the water molecules. For the ion−ion and ion−water interactions we have used a recent parametrization[31]—the so-called Madrid-2019 force field—based on the use of scaled charges and Lennard-Jones (LJ) short-range interactions for the ions. It includes parameters for all the ionic species present in our "in silico" seawater model (for simplicity we also assigned to the minor component the LJ parameters of the chloride ion). Ion−water and the more important ion−ion cross interactions were explicitly optimized. For the rest of the ion−ion cross interactions, the Lorentz−Berthelot combining rules were employed. Most of the systems are made of 15210 water molecules and the number of ions are multiples of the ISSS sample shown in Table 1. We have also studied a system at a lower salinity by considering the 318 ions of the ISSS sample and increasing the number of water molecules to 30 420.

The simulations have been performed using GROMACS 4.5.5[32] with a 2 fs time step. The cutoff radii have been set to 0.95 nm for the Lennard-Jones interactions. Long range corrections to the Lennard-Jones potential energy and pressure were included. Long range electrostatic interactions have been evaluated with the smooth Particle Mesh Ewald method.[12] The geometry of the water molecules and of the sulfate ions has been enforced using *ad hoc* constraints, in particular, the SHAKE algorithm. The Nosé−Hoover thermostat has been applied to set the temperatures at the desired values. All the simulations in the isobaric−isothermal (NpT) ensemble were performed at a fixed pressure of 1 bar by means of an isotropic Parrinello−Rahman barostat. The average volumes obtained in the NpT runs were used as input for the simulations at constant volume performed to evaluate the viscosities. The simulated time of the runs has been typically 10−20 ns for the calculation of the water−ions structure and residence times and, at least, 100 ns for the evaluation of viscosities, surface tension, ion diffusivities and ion−ion rdf's. Exceptionally a run of 500 ns has been carried out for the state at 15 °C, $S = 35.165$ g/kg in order to increase the accuracy of the diffusivity of the minor components.

The evaluation of some properties such as the density or the radial distribution function from a molecular dynamics run is trivial and may be found in textbooks.[12] However, the determination of other quantities still requires some methodological comments. For the evaluation of the viscosity we have used the Green−Kubo formula

$$\eta = \frac{V}{kT}\int_0^\infty \langle P_{\alpha\beta}(t_0)P_{\alpha\beta}(t_0 + t)\rangle_{t_0}\, dt \quad (1)$$

where $P_{\alpha\beta}(t)$ is a component of the pressure tension and the brackets $\langle\rangle$ denote the ensemble average. Some care is needed[33,34] to select the upper limit and the asymptotic value of the integral. The self-diffusion coefficients have been evaluated by means of the Einstein relation

$$D = \lim_{t\to\infty} \frac{1}{6t}\langle[\mathbf{r}_i(t) - \mathbf{r}_i(t_0)]^2\rangle \quad (2)$$

https://dx.doi.org/10.1021/acs.jctc.1c00072
J. Chem. Theory Comput. 2021, 17, 1715−1725

where $\mathbf{r}_i(t)$ and $\mathbf{r}_i(t_0)$ are the positions of the ith particle at time t and a certain origin of time t_0. For the calculation of the surface tension γ we considered a slab of liquid placed between two empty regions. In the case of a planar interface, γ is evaluated as

$$\gamma = \frac{L_z}{2}(\overline{p}_N - \overline{p}_T) \tag{3}$$

where $\overline{p}_N$ and $\overline{p}_T$ are the macroscopic normal and tangential components of the pressure tensor and L_z is the length of the simulation box along the direction perpendicular to the interface.

It is well-known that the truncation of the potential significantly affects the interfacial properties.[35] For the calculation of γ we have extended the cutoff radii r_c. At several salinities we have performed two sets of calculations using r_c = 1.3 nm and r_c = 1.6 nm and we have observed that the difference between the surface tension at a given salinity with respect to that for pure water $\gamma(S) - \gamma(0)$ is independent of the cutoff radii provided that both runs use the same cutoff. The values reported in this work correspond to simulations using r_c = 1.3 nm. The self-diffusion coefficients are also quite sensitive to finite-size effects,[36,37] but the size of our samples is already large enough to avoid this problem. In addition, it is expected that the error should cancel when we compare two values under identical conditions. Thus, $D(S)/D(0)$ is a more appropriate magnitude to investigate the diffusivity in seawater than $D(S)$ alone.

The hydration numbers, HN, are the average number of water molecules in the first solvation shell of an ion and are trivially obtained by integrating the corresponding water−ion rdf's. The residence times of these water molecules may be calculated from time correlation functions[38]

$$R(t) = \frac{1}{N_h}\sum_{i=1}^{N_h}[\Theta_i(0)\Theta_i(t)] \tag{4}$$

where $\Theta_i(t)$ is the Heaviside unit step function, which is 1 if a water molecule i is in the coordination shell of the ion at time t and zero otherwise, and N_h is the hydration number of this shell. From $R(t)$ it is possible to evaluate an average lifetime, τ, defined as

$$\tau = \int_0^\infty \langle R(t)\rangle \, \mathrm{d}t \tag{5}$$

Typically, $R(t)$ exhibits an exponential decay at short times, $R(t) \propto \exp(-t/\tau)$ so it can also be estimated from the corresponding fit.

The uncertainties of most of the quantities (with the exception of the viscosity) have been estimated from block averages.[39,40] The estimated error of the densities is very small, usually <0.02%, because the density is in most cases a byproduct of the calculation of the viscosity or the diffusion coefficients. The uncertainty of the viscosities has been estimated as the standard deviation of the results in the complete runs for each of the five independent pressure components.[33]

4. RESULTS

4.1. Results for the Madrid-2019 Force Field. In this section we compare the molecular dynamics results for the ISSS + water system with experimental measurements of Standard Seawater. Figure 1 shows that the calculated densities

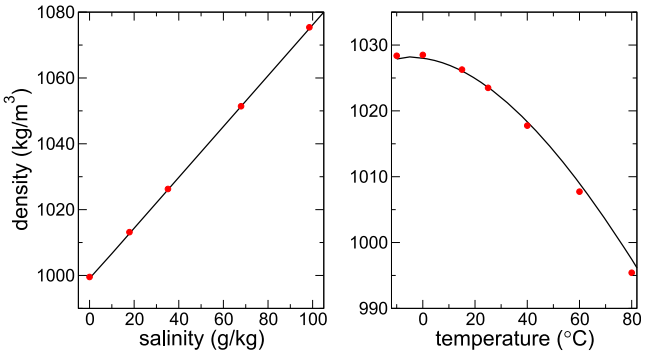

Figure 1. Comparison of the densities calculated in this work (points) with experimental data.[10] Left, as a function of salinity for seawater at 15 °C; right, as a function of temperature for seawater at S = 35.165 g/kg. The uncertainties are in all cases much smaller than the point size.

essentially match the experimental data and its dependence on salinity at 15 °C (close to the average temperature of the ocean surface waters). Notice that the salinity of the more concentrated solution in Figure 1 is about three times larger than the average salinity of open seas. As for the dependence of the density on temperature, we may observe in Figure 1 that the predictions of the "in silico" system are quite accurate for S = 35.165 g/kg. The simulation results show an excellent performance up to 40 °C, and the agreement between simulation and experiment degrades slightly at higher temperatures.

The results for the shear viscosity are presented in Figure 2. The simulation data reproduce adequately the dependence of

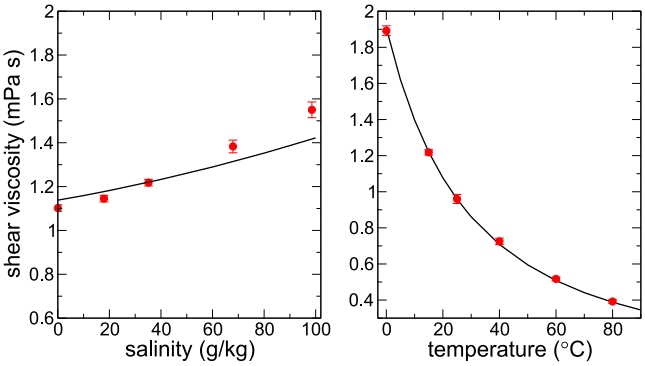

Figure 2. Comparison of the viscosities calculated in this work (points) with experimental data.[10] Left: as a function of salinity for seawater at 15 °C; right: as a function of temperature for seawater at S = 35.165 g/kg.

the viscosity on the salinity, though the slope of the curve is a bit steeper than that of the experimental values. Interestingly, the better agreement is found just for the more relevant seawater salinities region around 35 g/kg where experiment and numerical predictions are almost coincident. Figure 2 shows that the agreement extends over a wide range of temperatures. It is a fortunate coincidence that in addition to a generally excellent performance of the model, the better predictions correspond to temperatures and salinities around the average values of seawater in oceans.

The self-diffusion coefficient of the water molecules, D_w, in seawater of salinity S = 35.165 g/kg exhibits an almost perfect Arrhenius behavior in the range of temperatures from 0 to 80

https://dx.doi.org/10.1021/acs.jctc.1c00072
J. Chem. Theory Comput. 2021, 17, 1715−1725

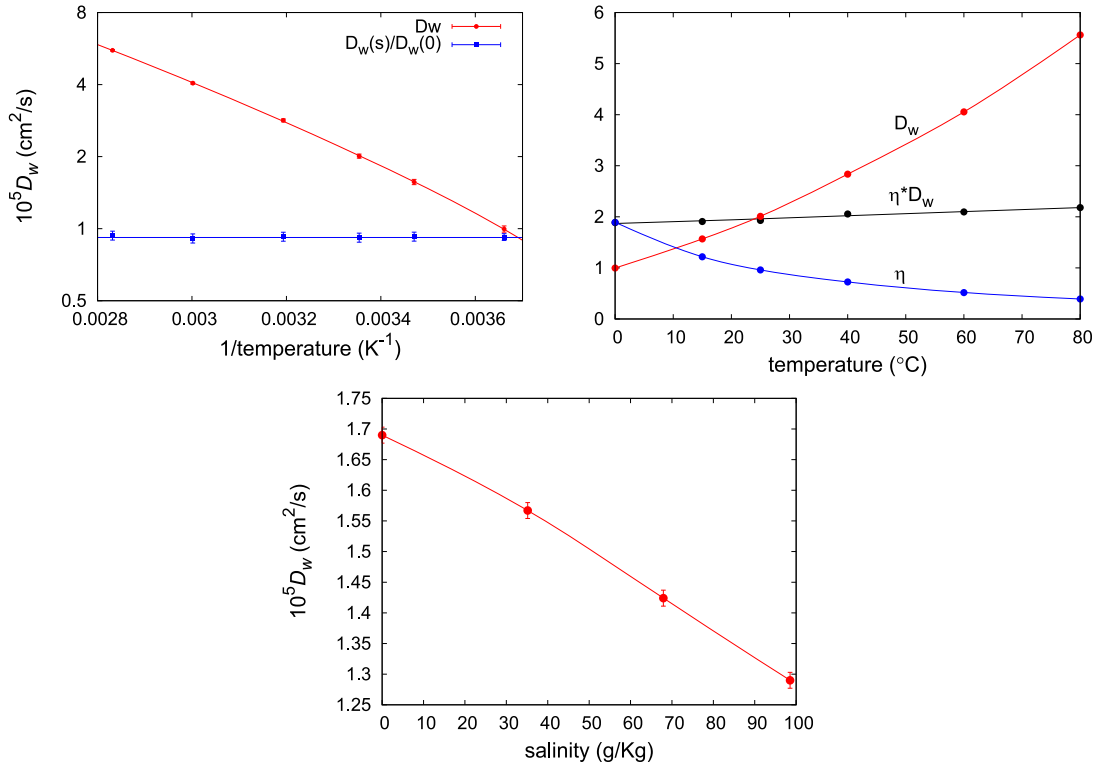

Figure 3. Top left: Self-diffusion coefficients of water as a function of the inverse of the temperature for "in silico" seawater at S = 35.165 g/kg in logarithmic scale (red circles). The blue symbols represent the ratio between the simulation values of the diffusion coefficients in seawater and those in simulations of pure water at the same temperature. Top right: Simulation values for D_w, η, and ηD_w as a function of temperature at S = 35.165 g/kg (units as in previous figures). Bottom: Self-diffusion coefficients of water as a function of salinity for seawater at 15 °C.

°C (see Figure 3). It is worth noting that the ratio between the diffusion coefficient in seawater and that for pure water at the same temperature seems to be independent of temperature, $D_w(S)/D_w(0) \approx 0.92$. It seems interesting to check whether a Stokes−Einstein-like (SE) equation is fulfilled in seawater using D_w as a proxy for the diffusion coefficient of the solution. The fractional SE coefficient t has been calculated from the relation $(D/T) \propto \eta^{-t}$. The result obtained from our values in the range of temperatures from 0 to 80 °C is t = 0.934, almost the same to the value t = 0.932 reported for TIP4P/2005 water in the interval 280−340 K.[41] It is interesting to note that, whereas the viscosity (and D_w) show a five times increase (decrease) in the 0−80 °C temperature range, the product ηD_w is almost constant (Figure 3). As for the dependence of D_w upon salinity, Figure 3 shows that the diffusion coefficients decrease with the salt concentration. The deviation from a linear decay is barely appreciable.

Figure 4 displays the self-diffusion coefficients of the ionic components of seawater in an Arrhenius-like plot. We have also included the rather scarce experimental measurements. The predictions for the "in silico" seawater model are semiquantitative. Since the simulation data seem to follow the experimental trend for all the ions, the results for Mg^{2+} are of particular importance because the usual radioactive tracer method for the experimental measurement of D can not be applied in this case. On the other hand, the agreement between experiment and simulation gives us some support to extrapolate the results to higher temperatures for which no experimental data have yet been reported. Notice finally that the self-diffusion coefficients follow approximately an Arrhenius behavior although the fitted curves seem to be slightly bended.

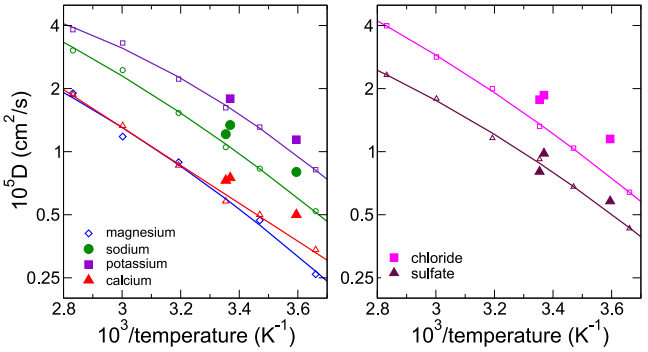

Figure 4. Self-diffusion coefficients of cations (left) and anions (right) as a function of the inverse of the temperature for seawater at S = 35.165 g/kg in logarithmic scale. Small symbols are the simulation results and large symbols are the experimental data.[42,43] Lines are a quadratic fit of the numerical results.

We now turn our attention to the structure of the solution. The difficulties of separating the contributions of each component make it extremely difficult to obtain the distribution functions from scattering experiments. The role of simulation in this case is complementary to experiment.

It is known that the hydration shell of the ions shows a weak dependence on salt concentration. Our results for seawater confirm this assertion. The position of the first extrema of a given ion−water rdf is the same, within the statistical uncertainty, in solutions at S = 35.165 and S = 98.56 g/kg. Only the heights of the peaks are slightly different. The

https://dx.doi.org/10.1021/acs.jctc.1c00072
J. Chem. Theory Comput. 2021, 17, 1715−1725

Table 2. Number of Water Molecules in the Hydration Shell (HN) of the Ionic Components of Seawater and Their Average Lifetimes, τ (in ps)[a]

	S = 35.165 g/kg				S = 98.56 g/kg			
ion	r_{min}	HN	τ_{integ}	τ_{decay}	r_{min}	HN	τ_{integ}	τ_{decay}
magnesium	0.315	6.00		1.4×10^5	0.315	6.00		0.9×10^5
calcium	0.325	7.45	114	116	0.322	7.45	118	119
sodium	0.315	5.53	18.2	18.6	0.316	5.53	19.4	20.0
sulfate	0.468	12.49	8.5	9.9	0.469	12.61	9.7	10.9
chloride	0.365	5.86	7.7	8.2	0.365	5.90	8.0	8.8
potassium	0.352	6.70	6.1	6.7	0.354	6.67	6.5	7.3

[a]HN is calculated by integrating the ion-O_w distribution functions up to the first minimum, r_{min} (in nm). τ_{integ} and τ_{decay} are the values of the residence times evaluated by integration of the autocorrelation function of HN and its fit to an exponential decay, respectively. Data correspond to simulations at 15 °C and two values of the salinity.

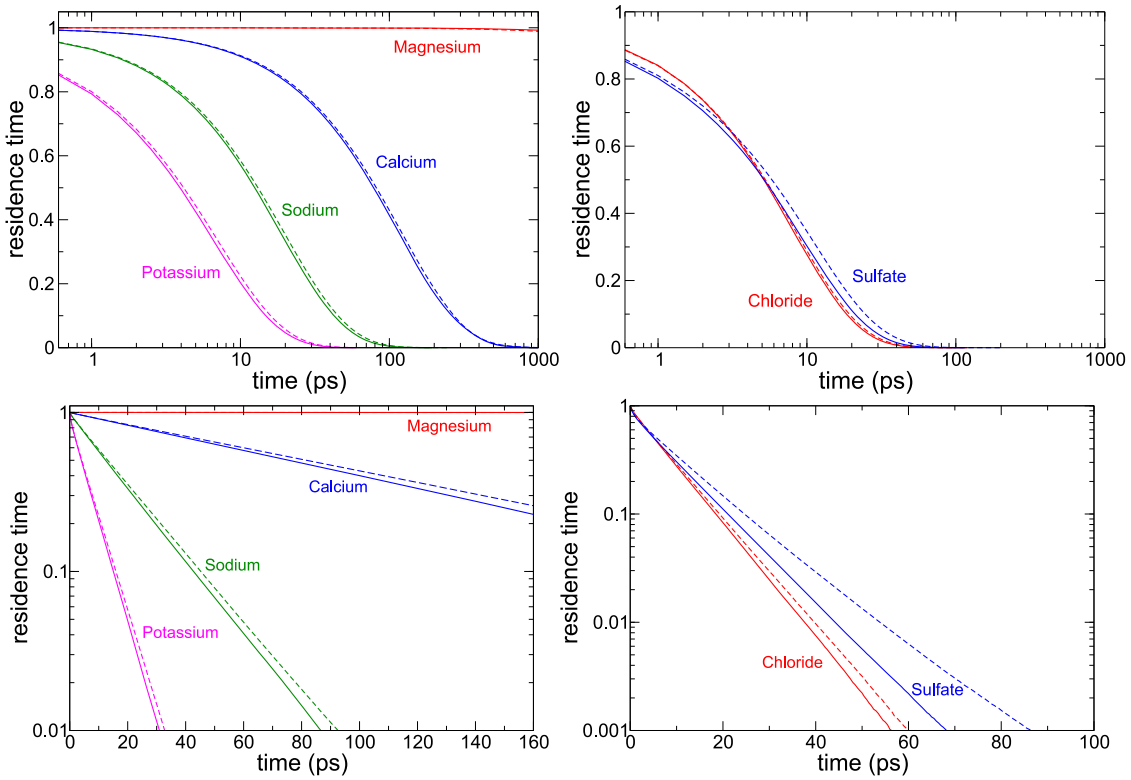

Figure 5. Residence times of water molecules in the hydration shell of the ions in seawater at 15 °C for two different salinities. Solid lines are the results at S = 35.165 g/kg and dashed lines correspond to S = 98.56 g/kg. In the top panels the time axis is represented on a logarithmic scale in order to obtain a better appreciation of the behavior at short and long times for all the ions in the same plot. In the bottom panels the lifetimes are represented on a logarithmic scale to illustrate the exponential decay behavior at short times.

hydration numbers are quite similar to those obtained for single salt electrolyte solutions at very high concentrations.[28,31] The HN results for the anions—see Table 2—seem to increase marginally with salinity while those of the cations seem to be independent of the salt content (the statistical uncertainty is below 0.01 for the magnesium ion and varies from 0.01 for the more abundant ions sodium and chloride to 0.04−0.05 for calcium and potassium).

Little is known about the residence time, $R(t)$, of the water molecules around ions. Our results are presented in Figure 5. The residence times are longer for the smaller ions. Since divalent cations are very small, waters around them are very tightly bound. In fact, the average lifetime of waters around magnesium ions is much longer than our simulation length so we may only estimate it by a fit of the autocorrelation function to an exponential decay. For cations carrying the same electronic charge, the ionic size increases with the atomic number so the residence times for calcium and potassium are smaller than those for magnesium and sodium, respectively. As expected, anions exhibit a looser hydration layer than cations. The large size of the sulfate anion motivates that, despite being a divalent ion, the lifetime of waters around sulfates is quite similar to that of chlorides. Finally, it is worth mentioning that the impact of a significant increase in the seawater salinity (by a factor of about three) results in a fairly small increase in the residence times.

Numerical values of the average lifetimes, τ, are given in Table 2. The values obtained using the short time exponential decay are quite similar to those obtained by integrating the correlation function though the difference between them is systematic. This seems to indicate that the behavior at longer times may deviate slightly from the exponential decay. The

https://dx.doi.org/10.1021/acs.jctc.1c00072
J. Chem. Theory Comput. 2021, 17, 1715−1725

order of magnitude of the τ's is qualitatively similar to those of a previous report for single salt aqueous solutions.[38] Quantitative differences are observed not only because of the use of different force fields but also because of the reduced simulation lengths in ref 38.

Given the complexity of the seawater composition, the number of radial distribution functions (rdf) is quite large so we only summarize here the more significant results. The presence of other ions, even if some of them are divalent, does not affect much the sodium-chloride rdf's. We will show below that the main features of the Na−Cl distribution functions, that is, location and height of the maxima and minima, are essentially the same as those of other aqueous solutions at similar concentrations. The situation may be different when dealing with less abundant species, especially when these are divalent ions.

In Figure 6 we compare the Mg−S distribution function in seawater at S = 35.1 g/kg to that of a solution containing only magnesium and sulfate ions at the same concentration (though, since magnesiums outnumber sulfates in seawater, some chloride anions must be added to enforce the charge balance). As seen in the plot the value of the Mg−S distribution function of the latter solution almost doubles that for seawater along a considerable range of distances. Only at distances around 2 nm do both curves cross and the coordination numbers of both solutions converge. This seems to be due to a shielding effect in seawater: the divalent magnesium ions attract unlike charged ions and, since the monovalent chloride ions are much more abundant than sulfates, some of the chlorides surround the magnesiums thus reducing their effective charge.

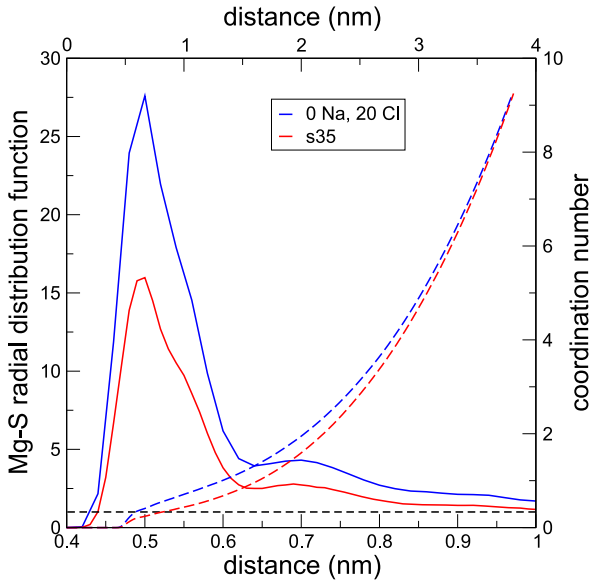

Figure 6. Mg−S(sulfate) radial distribution function (full lines) and running coordination numbers, n_c (dashed lines), for two solutions at 15 °C with the same number of water molecules, magnesium and sulfate ions (15210, 18, and 8, respectively). One of the systems is the ISSS + water solution at S = 35.165 g/kg and, thus, sodium, chloride, calcium, and potassium ions are present in the solution. The other system does not contain those ions with the exception of 20 chloride anions required to constrain the charge balance. The coordination number refers to the average number of magnesium cations in the first coordination shell of a sulfate. Notice that a different scale is used for the x-axis of the rdf (bottom) and n_c (top).

Figure 7 shows the increase in the surface tension of "in silico" seawater with respect to that of pure (TIP4P/2005) water as a function of salinity at 15 and 80 °C. The agreement with experimental results is excellent at oceanographic conditions. Also the variation with salinity is almost quantitatively predicted at 15 °C. As for the 80 °C isotherm, the agreement is only qualitative. The results follow the experimental trend but the gradient of the dependence on salinity is somewhat low, approximately $^3/_4$ of the experimental value for $\gamma(S) - \gamma(0)$.

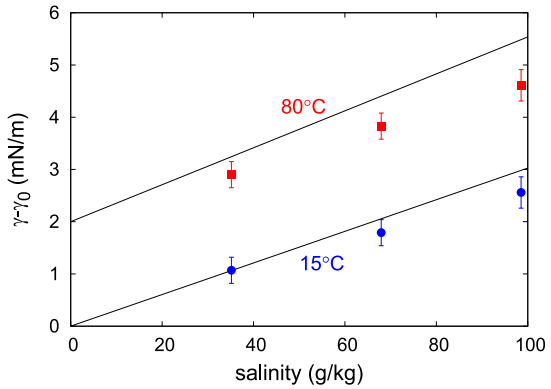

Figure 7. Surface tension of seawater relative to that of pure water. Symbols are the results for "in silico" seawater using TIP4P/2005 water as a reference; lines are experimental data.[44,45] Results at 80 °C have been shifted 2 mN/m for clarity.

4.2. Impact of Modifying the Number of Components of the Seasalt. One may wonder if the use of a more detailed representation of the seasalt composition might affect the quality of the results of this work. At this moment we cannot assess directly this point because there are no available parameters for other solutes compatible with those of the Madrid-2019 force field. However, we may obtain reasonable suggestions. Table 3 shows the results for the volumes calculated with the ISSS composition compared to those obtained when replacing the interactions of the calcium and potassium ions by those corresponding to magnesiums and sodiums, respectively ($ISSS_{318,4}$). Notice that the density of the solution is sensitive to the mass of the solute components but the volume is not. Thus, a comparison of the system volumes

Table 3. Volumes (in nm^3) for the ISSS Composition (See Table 1) Compared to Those of Solutions in Which the Potassium and Calcium Ions Are Replaced by Sodium and Magnesium Ions, Respectively ($ISSS_{318,4}$)[a]

t (°C)	salinity (g/kg)	ISSS	$ISSS_{318,4}$
−10	35.165	458.54	458.46
15	35.165	459.48	459.43
80	35.165	473.72	473.66
15	35.165	459.48	459.43
15	67.94	464.22	464.12
15	98.56	469.25	469.08

[a]All the systems contain 15210 water molecules so that S = 35.165 g/kg for the systems with 318 ions and six types of solutes. The systems at S = 67.94 g/kg (98.56 g/kg) contain the same number of water molecules but duplicate (triplicate) the number of ions in the sample.

https://dx.doi.org/10.1021/acs.jctc.1c00072
J. Chem. Theory Comput. 2021, 17, 1715−1725

provides an unambiguous test of the effect of replacing the interaction potential of a given ion by a different one. The differences between the results at S = 35.165 g/kg are very small, less than 0.1 nm^3 though larger than the combined statistical error (the estimated uncertainty of the results of a run is about 0.02 nm^3). The volumes for the ISSS$_{318,4}$ samples at S = 35.165 g/kg are systematically smaller than those of the ISSS ones but the differences are similar in the range of temperatures investigated. Increasing the salinity at constant temperature (15 °C) increases the departures between both sample sets. However, the differences remain quite small, the relative deviation being less than 0.04%. In summary, the substitution of potassium and calcium ions by cations with the same electric charge leads to an almost insignificant but detectable change of the system volume.

The repercussion of the simplification of the ionic sample on the shear viscosity is presented in Table 4. The estimated uncertainty of the results is less than 1.5%. Thus, the differences between the calculated viscosities of the ISSS and ISSS$_{318,4}$ samples are within the combined error of both simulations.

Table 4. Shear Viscosities (in mPa s) for the ISSS Composition (See Table 1) Compared to Those of Solutions Where the Potassium and Calcium Ions Are Replaced by Sodium and Magnesium Ions, Respectively[a]

t (°C)	salinity (g/kg)	ISSS	ISSS$_{318,4}$
15	17.90	1.145	1.125
15	35.165	1.22	1.23
15	67.94	1.38	1.37
15	98.56	1.55	1.57
−10	35.165	2.735	2.73
15	35.165	1.22	1.23
80	35.165	0.392	0.400

[a]The systems at S = 17.90 g/kg are composed of 318 ions and 30420 water molecules.

Figure 8 shows a comparison of the Na−Cl distribution functions for the ISSS and ISSS$_{318,4}$ systems at the same temperature and salinity. It may be seen that the rdf is almost insensitive to the modification of the salt composition. In fact, the difference respect to the rdf in a single salt NaCl solution is also barely appreciable. In summary, the presence of small amounts of additional ions has a negligible impact on the Na−Cl distribution function.

All the calculations for different properties indicate that the explicit incorporation of the calcium and potassium ions produces marginal changes with respect to the results obtained with a seawater sample containing only the four most abundant ions (chloride, sodium, magnesium, and sulfate). Notice that potassium and calcium are relatively abundant components of seawater; together they represent 1.8% of the sea salt mole fraction. Thus, the consequences of explicitly considering less abundant species such as the bicarbonate and bromide anions, which represent only a 0.2% of the sea salt, would be much more difficult to detect in molecular simulations. In fact, it is very likely that the impact of the incorporation of these ions to the simulated system would be comparable or even smaller than the uncertainty of the experimental measurements. Further increase of the composition details beyond the ISSS composition would only be strictly necessary if one intends to evaluate specific properties associated to a certain ion not included in the ISSS sample.

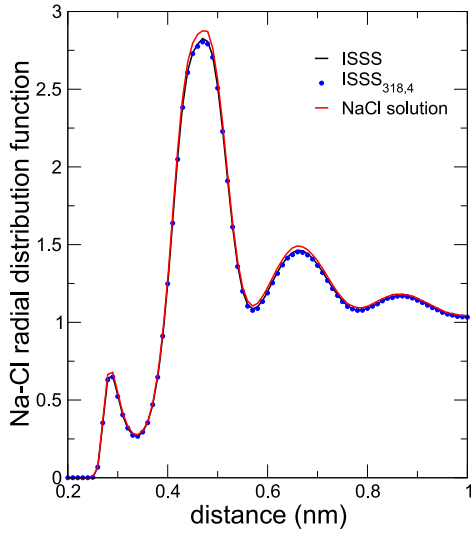

Figure 8. Na−Cl radial distribution function for the ISSS and ISSS$_{318,4}$ compositions at s = 35.165 g/kg. The curve labeled as Na−Cl refers to a pure NaCl solution with the same number of water molecules and occupying the same volume as the ISSS solution.

4.3. Comparison with the Results for Other Force Fields. In this section we compare the results for the Madrid-2019 force field with those obtained using an alternative set of parameters for the molecular interactions. Since a good model for water is of paramount importance we have also chosen TIP4P/2005[29] for the alternative force field. The more important components of seasalt are the sodium and chloride ions. The parameters for these ions have been taken from the work of Joung and Cheatham (JC), in particular those proposed for SPC/E water.[46] It has been shown that this is also an excellent choice when water is described by the TIP4P/2005 model.[47] For the sulfate anion we have selected the Cannon et al.[48] potential parameters. For the rest of the ionic solutes, we have employed the OPLS force field[49] as implemented in the Gromacs package. Lorentz−Berthelot combining rules were used for the cross interactions. For simplicity we shall denote this force field as JC.

The densities predicted by these force fields for a salinity S = 35.165 g/kg are shown in Figure 9. Overall the Madrid-2019 model performs better than JC. The predictions of the JC force field are noticeably different from the experimental densities at low to medium temperatures but the discrepancies decrease with increasing temperatures. Eventually, at 80 °C, the performance of the JC model is slightly better than that of the Madrid-2019 force field.

As for the shear viscosity, we observed the formation of calcium sulfate aggregates in the JC simulations. This may be expected considering that the concentrations of these ions in seawater are not far from the solubility limit of the salt. Increasing the Lorentz−Berthelot rules by a factor of 1.1 solved this issue (densities shown in Figure 9 were also obtained with this prescription). Figure 10 indicates that the performance of the Madrid-2019 force field is much better than that of the JC model at all the temperatures investigated for S = 35.165 g/kg.

https://dx.doi.org/10.1021/acs.jctc.1c00072
J. Chem. Theory Comput. 2021, 17, 1715−1725

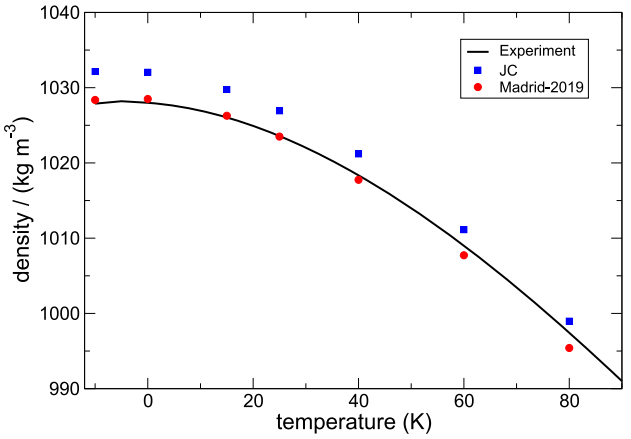

Figure 9. Density as a function of temperature for seawater at S = 35.165 g/kg using the Madrid-2019 and the JC force fields for the ions (see the text for details about JC). TIP4P/2005 is employed for water in both cases.

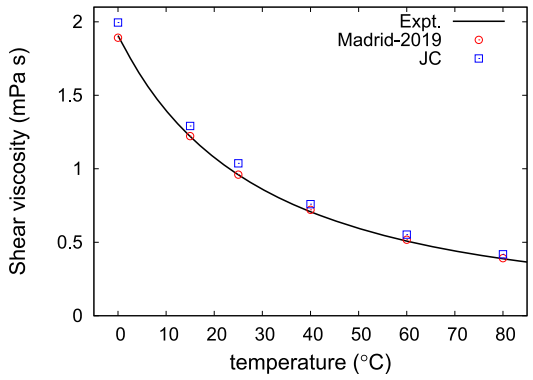

Figure 10. Shear viscosity as a function of temperature for seawater at S = 35.165 g/kg using the Madrid-2019 and the JC force fields for the ions and TIP4P/2005 for water (see the text for details.).

5. CONCLUSIONS AND FINAL DISCUSSION

We have shown in this work that molecular dynamics simulations of a solution mimicking the composition of seawater using a state of the art force field yield results in excellent agreement with experimental data. The quality of the predictions is particularly impressive in the oceanographic range but it is also very good for conditions relevant to desalination processes. It is difficult to assess at this moment the importance of this fact. Notice that the outcome of the simulation not only is a wide set of macroscopic properties but also gives detailed microscopic information which is sometimes very difficult to obtain in experiments. In this work we have calculated relevant magnitudes for which there is a large set of experimental determinations. It is the case of the density, viscosity or surface tension. The quality of the predictions validate the force field employed and our simplified representation of the seawater composition. This gives support to the predictions for structural quantities such as the hydration numbers and residence times of water molecules around ions as well as the ion−ion distribution functions. We have also obtained reliable results for the ionic diffusivity, a magnitude for which the experimental data are extremely scarce.

Once the force field has been verified, molecular simulation also allows performance of "what if?" pseudo-experiments. One may investigate the impact of small changes in composition by modifying the amount of any constituent. In fact, we have reported in this work the effect of replacing the calcium and potassium ions by magnesium and sodiums, respectively. Although we have limited our study to a seasalt containing only six types of ions, nothing prevents us, in principle, from extending our investigations to a more detailed composition. For instance, it would be very interesting to learn something about the behavior of the components involved in CO_2 sink in oceans[50] and CO_2 sequestration in deep saline aquifers.[51,52] The diffusion coefficient of CO_2 in brines has already been investigated by molecular simulation (see for instance ref 53.). However, similarly to the case of the salting out effect of methane[54] we have preliminary results indicating that the solubility of CO2 in a NaCl solution may not be described correctly by most of the current force fields. In addition, it would be necessary to fit the interaction parameters of CO2 with the main ionic components of seawater beyond standard LB rules. Although the design of appropriate force fields for them is not a trivial task, it is nowadays within our reach. In fact, we hope that this study will stimulate work in that direction.

■ ASSOCIATED CONTENT

Supporting Information

The Supporting Information is available free of charge at https://pubs.acs.org/doi/10.1021/acs.jctc.1c00072.

Description of the procedure to obtain optimal samples for the simulation of seawater. These samples reproduce as close as possible the Reference Composition with a minimum of solute molecules for a given number of components. Detailed table of the number of solute molecules in several optimal samples for up to 13 seasalt components (PDF)

■ AUTHOR INFORMATION

Corresponding Author

Jose L. F. Abascal − *Departamento de Química Física, Facultad de Ciencias Químicas, Universidad Complutense de Madrid, 28040 Madrid, Spain;* orcid.org/0000-0002-0304-3407; Email: abascal@ucm.es

Authors

Ivan M. Zeron − *Departamento de Química Física, Facultad de Ciencias Químicas, Universidad Complutense de Madrid, 28040 Madrid, Spain*

Miguel A. Gonzalez − *Departamento de Química Física, Facultad de Ciencias Químicas, Universidad Complutense de Madrid, 28040 Madrid, Spain*

Edoardo Errani − *Departamento de Química Física, Facultad de Ciencias Químicas, Universidad Complutense de Madrid, 28040 Madrid, Spain*

Carlos Vega − *Departamento de Química Física, Facultad de Ciencias Químicas, Universidad Complutense de Madrid, 28040 Madrid, Spain*

Complete contact information is available at: https://pubs.acs.org/10.1021/acs.jctc.1c00072

Author Contributions

‡I.M.Z. and M.A.G. contributed equally to this work

Notes

The authors declare no competing financial interest.

https://dx.doi.org/10.1021/acs.jctc.1c00072
J. Chem. Theory Comput. 2021, 17, 1715−1725

■ ACKNOWLEDGMENTS

This work has been funded by Grants PID2019-105898GB-C21 (Ministerio de Educación, Spain) and GR-910570 (UCM). I.M.Z. thanks CONACYT (México) for the financial support (Estancias Posdoctorales en el Extranjero) and M.A.G. acknowledges funding by Ministerio de Educacion, Spain (Juan de la Cierva fellowship, IJCI-2016-27497).

■ REFERENCES

(1) UNESCO. The International System of Units (SI) in Oceanography. *UNESCO Technical Papers in Marine Science* **1985**, 45.
(2) Marcet, A. J. G. On the specific gravity, and temperature of sea waters, in different parts of the ocean, and in particular seas; with some account of their saline contents. *Phil. Trans. R. Soc., London* **1819**, *109*, 161−208.
(3) Forchhammer, G. On the Constitution of Sea-Water, at Different Depths, and in Different Latitudes. *J. Franklin Inst.* **1865**, *79*, 107−109.
(4) Knudsen, M. On the standard-water used in the hydrographical research until July 1903. *ICES J. Mar. Sci.* **1903**, *s1*, 3.
(5) Millero, F. J.; Feistel, R.; Wright, D. G.; McDougall, T. J. The composition of Standard Seawater and the definition of the Reference-Composition Salinity Scale. *Deep Sea Res., Part I* **2008**, *55*, 50−72.
(6) Sandström, J. W. Dynamische versuche mit meerwasser. *Ann. Hydrograph. Maritimen Meteorol.* **1908**, *36*, 6−23.
(7) Rahmstorf, S. Thermohaline circulation: The current climate. *Nature* **2003**, *421*, 699.
(8) Rahmstorf, S. Ocean circulation and climate during the past 120,000 years. *Nature* **2002**, *419*, 207.
(9) IOC SCOR and IAPSO, The International Thermodynamic Equation of Seawater - 2010: Calculation and use of thermodynamic properties. *Intergovernmental Oceanographic Commission, Manuals and Guides*; IOC SCOR and IAPSO: 2010; Vol. *56*, p 220.
(10) Sharqawy, M. H.; Lienhard, J. H.; Zubair, S. M. Thermophysical properties of seawater: a review of existing correlations and data. *Desalin. Water Treat.* **2010**, *16*, 354−380.
(11) Roquet, F.; Madec, G.; Brodeau, L.; Nycander, J. Defining a simplified yet "realistic" equation of state for seawater. *Journal of Physical Oceanography* **2015**, *45*, 2564−2579.
(12) Frenkel, D.; Smit, B. *Understanding Molecular Simulation*; Academic Press: London, 1996.
(13) Debenedetti, P. G.; Sciortino, F.; Zerze, G. H. Second critical point in two realistic models of water. *Science* **2020**, *369*, 289−292.
(14) Corradini, D.; Rovere, M.; Gallo, P. A route to explain water anomalies from results on an aqueous solution of salt. *J. Chem. Phys.* **2010**, *132*, 134508.
(15) Zaragoza, A.; Tripathi, C. S. P.; Gonzalez, M. A.; Abascal, J. L. F.; Caupin, F.; Valeriani, C. Effect of dissolved salt on the anomalies of water at negative pressure. *J. Chem. Phys.* **2020**, *152*, 194501.
(16) Orozco, G. A.; Moultos, O. A.; Jiang, H.; Economou, I. G.; Panagiotopoulos, A. Z. Molecular simulation of thermodynamic and transport properties for the H2O+ NaCl system. *J. Chem. Phys.* **2014**, *141*, 234507.
(17) Jiang, H.; Mester, Z.; Moultos, O. A.; Economou, I. G.; Panagiotopoulos, A. Z. Thermodynamic and Transport Properties of H2O + NaCl from Polarizable Force Fields. *J. Chem. Theory Comput.* **2015**, *11*, 3802.
(18) Nezbeda, I.; Moučka, F.; Smith, W. R. Recent progress in molecular simulation of aqueous electrolytes: force fields, chemical potentials and solubility. *Mol. Phys.* **2016**, *114*, 1665−1690.
(19) Smith, W. R.; Nezbeda, I.; Kolafa, J.; Moučka, F. Recent progress in the molecular simulation of thermodynamic properties of aqueous electrolyte solutions. *Fluid Phase Equilib.* **2018**, *466*, 19−30.
(20) Baranyai, A. Alkali halide force fields: A search for an acceptable compromise. *J. Mol. Liq.* **2020**, *297*, 111762.
(21) Panagiotopoulos, A. Z. Simulations of activities, solubilities, transport properties, and nucleation rates for aqueous electrolyte solutions. *J. Chem. Phys.* **2020**, *153*, 010903.
(22) Leontyev, I. V.; Stuchebrukhov, A. A. Electronic continuum model for molecular dynamics simulations. *J. Chem. Phys.* **2009**, *130*, 085102.
(23) Leontyev, I. V.; Stuchebrukhov, A. A. Accounting for electronic polarization in non-polarizable force fields. *Phys. Chem. Chem. Phys.* **2011**, *13*, 2613−2626.
(24) Pluhařová, E.; Mason, P. E.; Jungwirth, P. Ion pairing in aqueous lithium salt solutions with monovalent and divalent counter-anions. *J. Phys. Chem. A* **2013**, *117*, 11766−11773.
(25) Kirby, B. J.; Jungwirth, P. Charge scaling manifesto: A way of reconciling the inherently macroscopic and microscopic natures of molecular simulations. *J. Phys. Chem. Lett.* **2019**, *10*, 7531.
(26) Kann, Z. R.; Skinner, J. L. A scaled-ionic-charge simulation model that reproduces enhanced and suppressed water diffusion in aqueous salt solutions. *J. Chem. Phys.* **2014**, *141*, 104507.
(27) Le Breton, G.; Joly, L. Molecular modeling of aqueous electrolytes at interfaces: effects of long-range dispersion forces and ionic charge rescaling. *J. Chem. Phys.* **2020**, *152*, 241102.
(28) Benavides, A. L.; Portillo, M. A.; Chamorro, V. C.; Espinosa, J. R.; Abascal, J. L. F.; Vega, C. A potential model for sodium chloride solutions based on the TIP4P/2005 water model. *J. Chem. Phys.* **2017**, *147*, 104501.
(29) Abascal, J. L. F.; Vega, C. A general purpose model for the condensed phases of water: TIP4P/2005. *J. Chem. Phys.* **2005**, *123*, 234505.
(30) Vega, C.; Abascal, J. L. F. Simulating water with rigid non-polarizable models: a general perspective. *Phys. Chem. Chem. Phys.* **2011**, *13*, 19663−19688.
(31) Zeron, I. M.; Abascal, J. L. F.; Vega, C. A force field of Li+, Na +, K+, Mg2+, Ca2+, Cl-, and SO4 2- in aqueous solution based on the TIP4P/2005 water model and scaled charges for the ions. *J. Chem. Phys.* **2019**, *151*, 134504.
(32) Hess, B.; Kutzner, C.; van der Spoel, D.; Lindahl, E. GROMACS 4: Algorithms for Highly Efficient, Load-Balanced, and Scalable Molecular Simulation. *J. Chem. Theory Comput.* **2008**, *4*, 435−447.
(33) Gonzalez, M. A.; Abascal, J. L. F. The shear viscosity of rigid water models. *J. Chem. Phys.* **2010**, *132*, 096101.
(34) Zhang, Y.; Otani, A.; Maginn, E. J. Reliable viscosity calculation from equilibrium molecular dynamics simulations: A time decomposition method. *J. Chem. Theory Comput.* **2015**, *11*, 3537−3546.
(35) Trokhymchuk, A.; Alejandre, J. Computer simulations of liquid/vapor interface in Lennard-Jones fluids: Some questions and answers. *J. Chem. Phys.* **1999**, *111*, 8510−8523.
(36) Yeh, I.-C.; Hummer, G. System-size dependence of diffusion coefficients and viscosities from molecular dynamics simulations with periodic boundary conditions. *J. Phys. Chem. B* **2004**, *108*, 15873−15879.
(37) Celebi, A. T.; Jamali, S. H.; Bardow, A.; Vlugt, T. J.; Moultos, O. A. Finite-size effects of diffusion coefficients computed from molecular dynamics: a review of what we have learned so far. *Mol. Simul.* **2020**, 1−15.
(38) Koneshan, S.; Rasaiah, J. C.; Lynden-Bell, R. M.; Lee, S. H. Solvent structure, dynamics, and ion mobility in aqueous solutions at 25 C. *J. Phys. Chem. B* **1998**, *102*, 4193−4204.
(39) Hess, B. Determining the shear viscosity of model liquids from molecular dynamics simulations. *J. Chem. Phys.* **2002**, *116*, 209−217.
(40) Gonzalez, M. A.; Valeriani, C.; Caupin, F.; Abascal, J. L. F. A comprehensive scenario of the thermodynamic anomalies of water using the TIP4P/2005 model. *J. Chem. Phys.* **2016**, *145*, 054505.
(41) Tsimpanogiannis, I. N.; Jamali, S. H.; Economou, I. G.; Vlugt, T. J. H.; Moultos, O. A. On the validity of the Stokes−Einstein relation for various water force fields. *Mol. Phys.* **2020**, *118*, No. e1702729.
(42) Yuan-Hui, L.; Gregory, S. Diffusion of ions in sea water and in deep-sea sediments. *Geochim. Cosmochim. Acta* **1974**, *38*, 703−714.

https://dx.doi.org/10.1021/acs.jctc.1c00072
J. Chem. Theory Comput. 2021, 17, 1715−1725

(43) Poisson, A.; Papaud, A. Diffusion coefficients of major ions in seawater. *Mar. Chem.* **1983**, *13*, 265−280.
(44) Nayar, K. G.; Panchanathan, D.; McKinley, G. H.; Lienhard, J. H. Surface Tension of Seawater. *J. Phys. Chem. Ref. Data* **2014**, *43*, 043103.
(45) Vinš, V.; Hykl, J.; Hrubgrỳ, J. Surface tension of seawater at low temperatures including supercooled region down to −25 C. *Mar. Chem.* **2019**, *213*, 13−23.
(46) Joung, I. S.; Cheatham, T. E. Determination of alkali and halide monovalent Ion Parameters for Use in Explicit Solvated Biomolecular Simulation. *J. Phys. Chem. B* **2008**, *112*, 9020.
(47) Dopke, M. F.; Moultos, O. A.; Hartkamp, R. On the transferability of ion parameters to the TIP4P/2005 water model using molecular dynamics simulations. *J. Chem. Phys.* **2020**, *152*, 024501.
(48) Cannon, W. R.; Pettitt, B. M.; McCammon, J. A. Sulfate anion in water: model structural, thermodynamic, and dynamic properties. *J. Phys. Chem.* **1994**, *98*, 6225−6230.
(49) Jorgensen, W. L. In *Encyclopedia of Computational Chemistry*; von, R., Schleyer, P., Ed.; John Wiley and Sons: 1998; Vol. *3*.
(50) Feely, R. A.; Sabine, C. L.; Lee, K.; Berelson, W.; Kleypas, J.; Fabry, V. J.; Millero, F. J. Impact of anthropogenic CO2 on the CaCO3 system in the oceans. *Science* **2004**, *305*, 362−366.
(51) Celia, M. A.; Bachu, S.; Nordbotten, J. M.; Bandilla, K. W. Status of CO2 storage in deep saline aquifers with emphasis on modeling approaches and practical simulations. *Water Resour. Res.* **2015**, *51*, 6846−6892.
(52) Shi, Z.; Wen, B.; Hesse, M.; Tsotsis, T.; Jessen, K. Measurement and modeling of CO2 mass transfer in brine at reservoir conditions. *Adv. Water Resour.* **2018**, *113*, 100−111.
(53) Garcia-Rates, M.; de Hemptinne, J.-C.; Avalos, J. B.; Nieto-Draghi, C. Molecular modeling of diffusion coefficient and ionic conductivity of CO2 in aqueous ionic solutions. *J. Phys. Chem. B* **2012**, *116*, 2787−2800.
(54) Blazquez, S.; Zeron, I. M.; Conde, M. M.; Abascal, J. L. F.; Vega, C. Scaled charges at work: Salting out and interfacial tension of methane with electrolyte solutions from computer simulations. *Fluid Phase Equilib.* **2020**, *513*, 112548.

https://dx.doi.org/10.1021/acs.jctc.1c00072
J. Chem. Theory Comput. 2021, 17, 1715−1725